

Article

Exploring the Impact of Vehicle Lightweighting in Terms of Energy Consumption: Analysis and Simulation on Real Driving Cycle

Giulia Sandrini , Daniel Chindamo , Marco Gadola , Andrea Candela and Paolo Magri 

Department of Mechanical and Industrial Engineering, University of Brescia, 25123 Brescia, Italy; daniel.chindamo@unibs.it (D.C.); marco.gadola@unibs.it (M.G.); andrea.candela@unibs.it (A.C.); p.magri003@unibs.it (P.M.)

* Correspondence: giulia.sandrini@unibs.it

Abstract: Today, reducing vehicle energy consumption is a crucial topic. For electric vehicles, reducing energy consumption is essential to address some of the most critical issues associated with this type of vehicle, such as the limited range of electric powertrains and the long battery recharging times. To lower the environmental impact during the vehicle's use phase and reduce energy consumption, vehicle mass reduction (lightweighting) is an effective strategy. The objective of this work is to analyze the vehicle parameters that influence lightweighting outcomes on a real driving cycle, representative of the home-to-work travel in northern Italy. In particular, a previous work carried out on standard driving cycles is repeated in order to observe whether it is possible to draw the same conclusions regarding the variability in the lightweighting outcome. This study was conducted using two opposite vehicle models, a compact car and an N1 vehicle, simulated through a well-established vehicle simulation tool for energy consumption estimation. To conduct this analysis, several simulations with variable vehicle mass, and with different vehicle parameters, such as aerodynamics and rolling resistance, were performed to estimate energy consumption across a real-world driving cycle, acquired via GPS on board the vehicle during a home-to-work journey in northern Italy. This study reveals that even for the real driving cycle, as for the WLTC and US06 standards, the parameters that most influence the outcome of the lightening are the rolling resistance, the characteristics of the battery pack, the aerodynamic coefficients, and the efficiency of the transmission. Finally, the standard cycle that best fits with the real one considered in this study is the Artemis Urban Cycle.

Keywords: vehicle lightweighting; automotive; energy consumption; consumption analysis; fuel reduction value (FRV); energy reduction value (ERV); real driving cycle; real data



Citation: Sandrini, G.; Chindamo, D.; Gadola, M.; Candela, A.; Magri, P. Exploring the Impact of Vehicle Lightweighting in Terms of Energy Consumption: Analysis and Simulation on Real Driving Cycle. *Energies* **2024**, *17*, 6398. <https://doi.org/10.3390/en17246398>

Academic Editor: Chunhua Liu

Received: 29 October 2024

Revised: 26 November 2024

Accepted: 17 December 2024

Published: 19 December 2024



Copyright: © 2024 by the authors. Licensee MDPI, Basel, Switzerland. This article is an open access article distributed under the terms and conditions of the Creative Commons Attribution (CC BY) license (<https://creativecommons.org/licenses/by/4.0/>).

1. Introduction

The issue of reducing consumption has become highly significant today, both for internal combustion vehicles and electric vehicles. Fuel efficiency is especially crucial for internal combustion engines due to the concerns about emissions and the strict regulations surrounding them [1–3]. On the other hand, for electric vehicles, minimizing energy consumption is key to addressing some of their most pressing challenges, particularly the limited driving range and the long battery recharging times [4].

A useful technique to reduce the impacts in the use phase and the fuel or energy consumption of vehicles [5,6] is to reduce the mass of the vehicle [7–12]. This process is commonly referred to as “vehicle lightweighting” in the automotive field.

Vehicle lightweighting can be achieved in different ways: through material substitution and design and construction changes, using lighter materials, while maintaining the required strength characteristics [5,9,13–17]; minimizing the size of the battery pack adopting alternative/hybrid powertrains [18,19]; ad hoc regenerative braking logics and

range management logics [20,21]; and/or improving battery efficiency, for example, by changing their chemistry [20] or studying alternative battery cooling systems [22].

Numerous scientific studies, such as [7,23–26], present the outcomes of vehicle lightweighting using the Fuel Reduction Value (FRV), which is measured in L/(100 km·100 kg). In the context of internal combustion vehicles, the FRV index stands for the liters of gasoline or diesel saved every 100 km, resulting from a 100 kg reduction in vehicle mass.

However, when referring to electric vehicles, consumption is no longer referred to as fuel consumption but the variation in energy stored in the battery pack. If a study is then conducted using the FRV index, as in the case of [26], the latter index will represent the equivalent liters per 100 km and per 100 kg of lightweighting. An alternative is to analyze the lightweighting outcome on the basis of the Energy Reduction Value (ERV) index, expressed in kWh/(100 km·100 kg), which corresponds to the energy savings every 100 km for every 100 kg of mass reduction. Studies [27–29] use the ERV coefficient, and, in particular, ref. [29] considers the FRV index for the internal combustion vehicles and the ERV index for electric vehicles.

Scientific papers [24,25] show how the FRV coefficient changes based on the vehicle class considered, therefore depending on the size/volume of the vehicle considered. However, they do not identify the specific vehicle parameters responsible for this variation; in this way, it might seem that this change is simply due to the variation in the vehicle weight. In contrast, the focus of [28] is the research and analysis of the vehicle parameters that influence the lightweighting results of electric vehicles, thus considering the ERV index.

However, a study [28] was conducted on standardized driving cycles, in particular on the WLTC and on the US06 cycles, finally comparing the outcome of the vehicle lightweighting obtained on different standard driving cycles and showing how this outcome varies according to the cycle considered. What is missing from the work presented in [28] is the analysis of the parameters that influence the lightweighting result based on a real-world driving cycle.

Non-legislative driving cycles are widely used in research focused on energy efficiency and pollution assessment. For this reason, several authors address the problem of how to obtain driving cycles that are representative of reality [30–36]. These non-legislative cycles have been utilized in studies covering topics from performance prediction to vehicle design [37]. In fact, vehicle emissions are influenced by driving cycles, which are primarily determined by traffic conditions [38]. Given the possible strong variability in local traffic, or from city to city, for the same geographical area, the standardized driving cycles often cannot be representative of all cases [37].

This paper is therefore focusing on the use of a real-world driving cycle to estimate the impact of vehicle lightweighting, considering the north of Italy as the reference working area, specifically the province of Brescia, in the Lombardy region. In this regard, the outcome of the lightweighting has been evaluated on a real-world cycle acquired on board the vehicle equipped with a GPS antenna, on a representative home-to-work journey, from a town in the province of Brescia, crossing the city center, up to the north of the municipality of Brescia.

Finally, the results obtained using the real-world driving cycle were compared with those coming from different standard cycles to try and establish which standard driving cycle is more representative of the chosen case (northern Italy, Lombardy region, home-to-work journey from the province to the municipality of Brescia) [39].

In this work, it has been found that in order to achieve an accurate calculation of the ERV index it is crucial to correctly define the rolling resistance coefficient, the aerodynamics coefficients, the battery pack parameters, and the transmission efficiency for both the real-world driving cycle and the standardized driving cycles, while the inertia contribution can be considered negligible. Finally, it has been also found that the standardized driving cycle that best fits the real-world scenario is the Artemis Urban Cycle.

This paper is organized as follows:

- Section 2 outlines the adopted methodology, detailing the reference vehicles used in this study, the reference real driving cycle, the simulation tool utilized, the vehicle parameters under investigation, and a brief description of the simulations conducted;
- Section 3 presents the results of this study and the considerations derived from them;
- Section 4 discusses and organizes the results presented in Section 3;
- Section 5 provides concluding remarks, summarizes the most relevant information from Section 4, and proposes future works.

2. Materials and Methods

The aim of this study is to assess the vehicle parameters that affect the outcomes of lightweighting, considering vehicle categories M1 and N1 [40]. To conduct this analysis, several simulations with variable vehicle mass were performed using the last version of the model described in [41] to estimate the energy consumption across a real driving cycle, representative of the geographical context considered: northern Italy, Lombardy region, province of Brescia.

2.1. Reference Vehicles

For this work, the same reference vehicles as in study [28] were considered, i.e., two opposite vehicle types: a utility compact car (segment B) of the M1 category, and a light commercial vehicle of the N1 category. The B segment vehicle is the consolidated “CompactCar” model from VI-CarRealTime (VI-Grade), but without an endothermic engine and with an electric driveline of the “Fiat 500e Hatchback 42 kWh” instead [42,43], a popular car in Italy and Europe, characterized by an 87 kW electric motor, a single reduction transmission ratio of 9.6, and a 42 kWh battery pack. On the other hand, the N1 category vehicle is the same one used in [41] for the validation of the tool during simulations of low-performance vehicles but with a total transmission ratio of 6.22.

For the two vehicle models (compact car of M1 category and N1 vehicle), Table 1 reports the model parameters used for the purpose of this study.

Table 1. Model parameters used for the purpose of this study, for the compact car (M1 category) and for the N1 category vehicle [28].

Analyzed Parameters	Compact Car Value	N1 Value
Transmission efficiency	1	0.9409
Af · Cx *	1.034 m ²	2.1 m ²
Vertical aerodynamic coefficient	−0.026 m ²	0
Rolling friction coefficient	0.01	0.015
Total gear ratio	9.6	6.22
Front wheel radius	0.2987 m	0.35 m
Rear wheel radius	0.3005 m	0.35 m
Moment of inertia of each wheel	0.882 kg m ²	1.09 kg m ²
Moment of inertia of the motor	0.02 kg m ²	0.086 kg m ²
Moment of inertia of the transmission	0.0001 kg m ²	0.01 kg m ²
Battery capacity	42 kWh (105 Ah)	120 Ah
Number of battery cells in series	96	108
Number of battery cells in parallel	2	1
Nominal battery pack voltage	400.0 V	356.1 V
Internal resistance of the battery pack	0.086 Ω	0.097 Ω

* Frontal area (Af) multiplied by longitudinal aerodynamic coefficients (drag, Cx).

It was chosen to simulate the two vehicle models without regenerative braking to prevent the results from being influenced by regenerative braking logic with different behaviors depending on the vehicle considered.

2.2. Driving Cycle

For this study, a real-world driving cycle was considered, representing a home-to-work journey for all the people who live in northern Italy, commuting from the province and crossing the city to reach their workplace.

For the driving cycle acquisitions, a GPS antenna connected to a MoTeC (Melbourne, Australia) ADL2 [44] data acquisition system was used. The GPS receiver is a LOCOSYS (New Taipei City, Taiwan)—LS23036 [45], with an update rate of up to 10 Hz and a position accuracy of 2.5 m. Figure 1 shows the installation position of the GPS receiver and the location in the vehicle of the data acquisition system.



Figure 1. Location (a) of the GPS receiver (red circle), installed on the vehicle hood via magnetic connection, and (b) of the MoTeC ADL2 data acquisition unit, on the passenger mat, inside a protective box.

The vehicle used is a Suzuki (Hamamatsu, Shizuoka, Japan) Jimny, which is a light-duty vehicle model (N1) from 2021. The vehicle weight is 1065 kg (empty weight); it is powered by petrol with a nominal engine power of 102 CV (75 kW). It is equipped with a 4WD 5-gear transmission and with reduced gears. The measurements were carried out with the gearbox in standard mode (reduced gear and 4WD disengaged).

With this vehicle, equipped with the MoTeC ADL2/GPS data acquisition system, several driving cycles including the speed profile, the altitude profile, and other information were acquired. Among all the trips, the most representative journey was chosen (see Figure 2), excluding those characterized by extraordinary events that rarely occur, for example, heavy rain, strong wind, stops at petrol stations, emergency braking with activation of the ABS system, roadworks, etc.

The chosen reference real-world driving cycle was acquired on 16 May 2024 from 8:15 to 9:15 a.m., starting from the province of Brescia, from a place located between the towns of Gambara and Gottolengo, and arriving at the engineering faculty of the University of Brescia. This route includes crossing the Brescia city center during the time of day with the highest level of traffic. The acquired speed profile, reported in Figure 3, is characterized by many phases at zero speed, a maximum speed of 100.5 km/h, and an average speed of 36.1 km/h.

The reference real-world driving cycle is a mixed cycle, urban and extra-urban, and in this journey, approximately 40 min are spent at speeds below 50 km/h and approximately 18 min are spent at speeds between 50 and 90 km/h, while only about 1 min is spent at speeds above 90 km/h. For more information, see also Figure 4.

GPS systems are known to provide accurate longitude and latitude data, while they typically provide imprecise altimetric information. For this reason, it was decided to use software available on the web, “GPS Visualizer” [46], to obtain a more precise altimetric profile of the real cycle acquired. This tool allows for obtaining altimetric data starting from latitude and longitude data, using different DEM (Digital Elevation Model) sources. In particular, it is possible to set “GPS Visualizer” so that it automatically uses the best source

among various DEMs. The altimetry profile obtained is reported in Figure 5 and compared to the profile acquired directly with the GPS on board the vehicle.

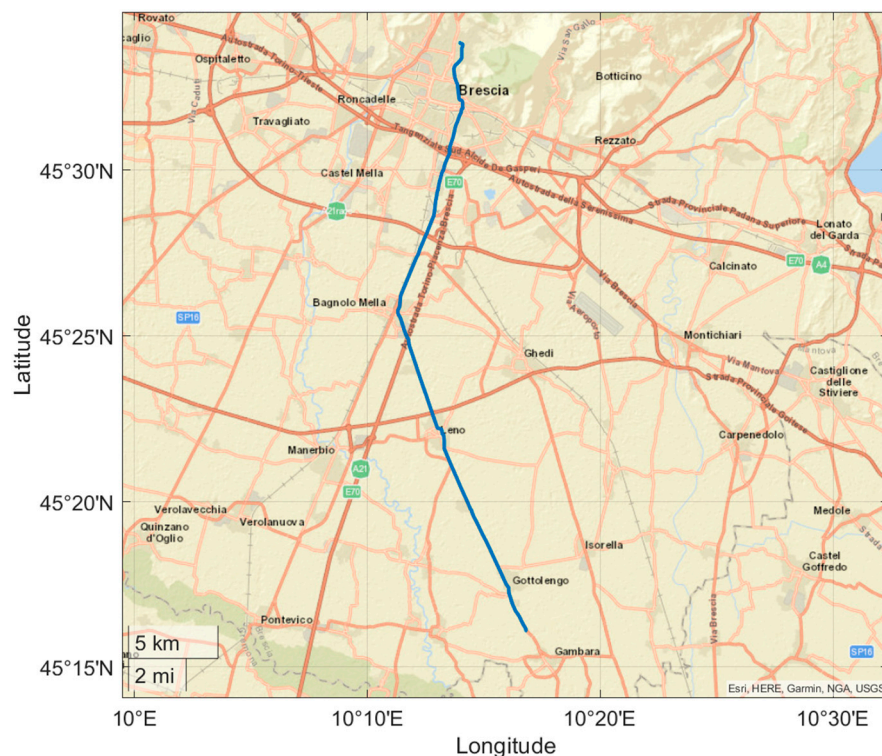


Figure 2. Home-to-work commute real-world reference driving cycle.

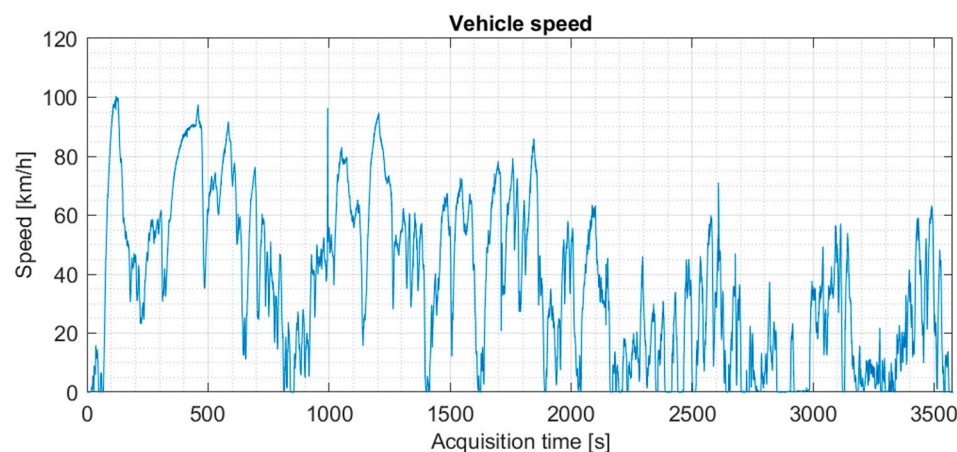


Figure 3. Acquired speed profile of the reference real driving cycle.

The effects of lightweighting on a real driving cycle, for both reference vehicles, were compared with the following standard driving cycles:

- WLTC (Worldwide Harmonized Light-Duty Vehicles Test Cycle), class 3b, described in the WLTP (Worldwide Harmonized Light-Duty Vehicles Test Procedure) procedure [47];
- SFTP-US06, described in the “EPA Supplemental Federal Test Procedure” (SFTP) [48];
- FTP75 (EPA Federal Test Procedure) [49];
- HWFET (EPA Highway Fuel Economy Cycle);
- Japanese JC08 Emission Test Cycle [50], with a first additional phase equal to the phase corresponding to the last 172 s of the standard JC08 cycle itself;
- Artemis Urban, Rural Road, and Motorway (130) cycles [51].

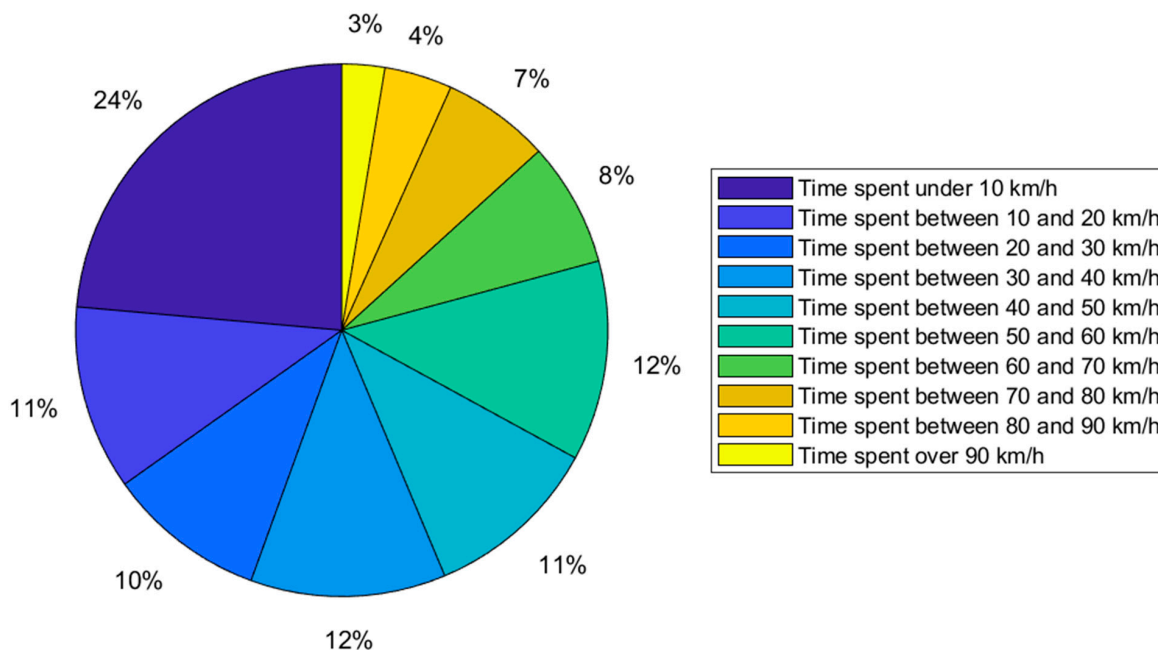


Figure 4. Time spent at different vehicle speed ranges, as a percentage of total travel time (about 59.67 min).

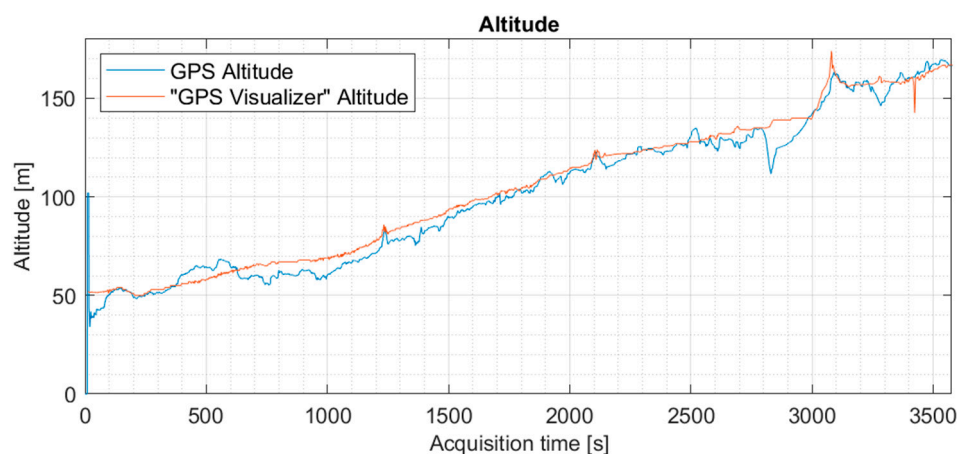


Figure 5. Altimetry profile obtained through the “GPS Visualizer” [46] tool using GPS latitude and longitude vs. altimetry profile directly acquired from GPS on board the vehicle.

Table 2 provides the comparative characteristics of the studied driving cycle, according to the following parameters: the maximum and average speed; maximum acceleration; and idling time, expressed as a percentage fraction of the total cycle time.

Table 2. Driving cycles’ characteristics.

Driving Cycle	Maximum Speed [km/h]	Average Speed [km/h]	Maximum Acceleration [m/s ²]	Idling Time [%]
Reference real driving cycle	100.5	36.1	1.9 *	6.7
WLTC—Class 3b	76.6	27.7	1.7	13.1
US06	80.3	77.3	2.3	7.5
FTP75	91.2	12.2	1.5	19.1
HWFET	96.4	77.7	1.4	0.8
JC08	81.6	27.0	1.7	27.1

Table 2. Cont.

Driving Cycle	Maximum Speed [km/h]	Average Speed [km/h]	Maximum Acceleration [m/s ²]	Idling Time [%]
Artemis—Urban Cycle	57.7	17.7	2.9	28.4
Artemis—Rural Road Cycle	111.5	57.5	2.4	3.0
Artemis—Motorway Cycle (130)	131.8	96.9	1.9	1.5

* Value obtained from simulations in order to exclude speed peaks caused by GPS detection errors.

2.3. Simulation Tool

For the simulation, the last version of the TEST (Target-speed EV Simulation Tool) model [41] was used. This is a vehicle longitudinal dynamics simulation tool that enables the simulation of both the mechanical and electrical behaviors of fully electric or hybrid electric vehicles. The model is presented in [41], and the latest version of the latter, adopted in [28], was used.

2.4. Parameters of the Vehicle (And of Its Model) That Can Affect the Lightweighting Results

In this study, the variability of the outcome given by the lightweighting was analyzed as a function of the variation in the same parameters considered in [28], as follows:

- Battery pack parameters (the nominal voltage, capacity, and internal resistance);
- Aerodynamic parameters;
- Transmission efficiency;
- Rolling resistance, in particular changing the rolling friction coefficient;
- Moments of inertia of the electric motor, of the rotating parts of the transmission, and of the wheels;
- Total transmission ratio (including the wheel ratio given by the wheel radius).

Finally, the driving cycle considered is also a fundamental parameter to take into account; therefore, the results obtained considering the real-world driving cycle were compared with those obtained on different standardized driving cycles.

2.5. Set of Simulations

In this study, “set of simulations” (or “simulation set”) means the collection of simulations, conducted for the same driving cycle and for the same vehicle model, differentiated only by the mass of the vehicle. In particular, for the compact car models, the simulations were carried out starting from 700 kg, up to 2500 kg, for every 50 kg of variation in vehicle weight. For the N1 vehicle, it was always every 50 kg but from 700 kg up to 3500 kg, which corresponds to the maximum permitted weight for light commercial vehicles. For a commercial vehicle, 700 kg is unrealistic, but the simulations were pushed up to this value for an easier comparison with the results of the compact car.

A first set of simulations for each reference vehicle model (compact car and N1) was obtained by providing the real-world speed profile acquired via GPS as input to the TEST model and, for each single simulation, by varying the mass of the vehicle under examination. Then, these sets of simulations were initially repeated by setting all the inertia contributions of the two vehicle models to zero.

Further sets of simulations, always based on the real driving cycle, instead concern the compact car, in which one or more parameters were modified to make them equal to those of the reference N1 category vehicle. The modified parameters for each simulation set are as follows:

- Battery pack parameters (the nominal voltage, capacity, and internal resistance);
- Aerodynamics;
- Transmission efficiency;
- Rolling friction coefficient;
- Moments of inertia (of the motor, transmission, and wheels);
- All the previous parameters simultaneously;

- Motor reduction ratio, transmission ratio, and wheel radii;
- All of the above parameters simultaneously.

Finally, for this work, the simulation sets obtained for study [28] were considered, in particular relating to the compact car and N1 models, without regenerative braking, on the standard cycles reported at the end of Section 2.2. These simulations were finally compared with those obtained on the real driving cycle covered by this study.

3. Results

This section presents the results of the simulation sets conducted, with consequent considerations.

3.1. Consumption Analysis

Figure 6 shows the results of the simulation sets obtained for the compact car and N1 vehicle models, with and without inertia contributions. In particular, the results are reported in terms of average energy consumption over the real-world cycle as a function of vehicle weight.

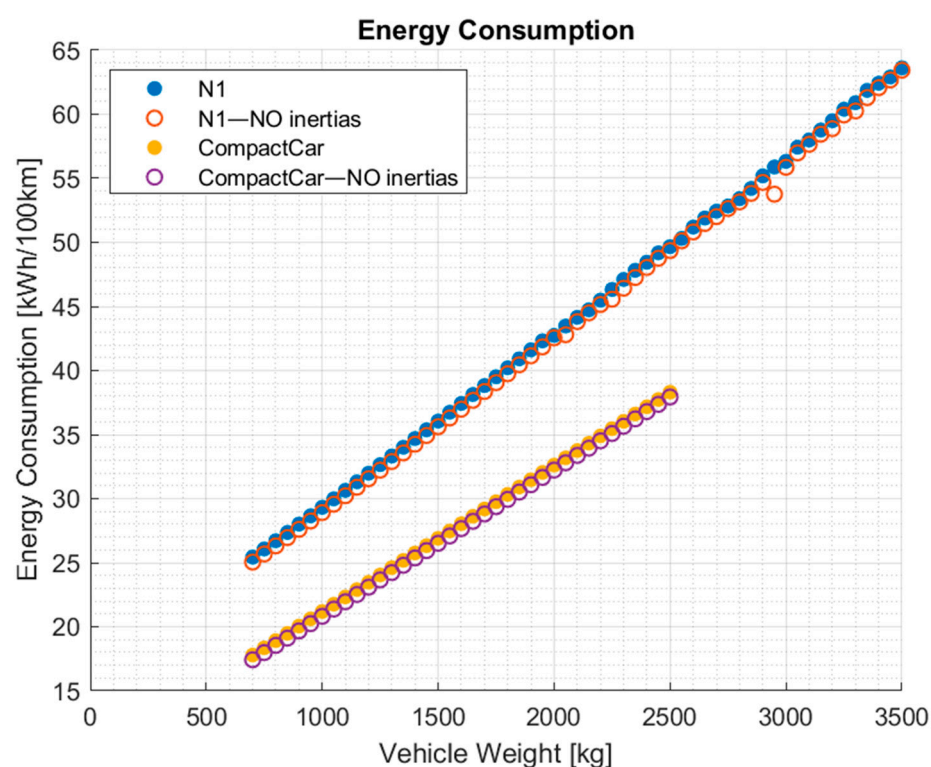


Figure 6. Average energy consumption over the reference real driving cycle, as a function of vehicle weight, for the N1 category vehicle model (“N1”) and for the same model but with zero inertia contributions (“N1—NO inertias”); for the compact car model (“CompactCar”); and for the same model but with zero inertia contributions (“CompactCar—NO inertias”).

From Figure 6, the inertia can be considered negligible, as obtained for study [28] for the WLTC and US06 standard driving cycles. Even in the case of this real driving cycle, it is therefore possible to ignore the inertia contributions when building a vehicle model to be adopted for the analysis of the outcome of the lightweighting.

In Figure 6, it is also possible to see that there is an error for the consumption result for the simulation on the N1 model without an inertia contribution, with the vehicle weight equal to 2950 kg. In fact, this consumption value is not aligned with the other data trend.

This issue arises primarily because the vehicle, at higher weights, struggles to meet the speed target around 994 s after the start of the simulation, due to the excessively high

acceleration demands caused by a speed spike due to a GPS detection error. In this regard, Figure 7 shows a comparison between the target speed and the vehicle speed during the simulation, for a vehicle weight of 2950 kg and without inertia contributions. In fact, as can be observed in Figure 8, the high acceleration of that stretch leads to a high torque request, which cannot be satisfied by the vehicle under examination. A torque limit of 10,000 Nm was implemented in the simulation model to enable the vehicle to follow the imposed speed profiles without encountering restrictions. However, this limitation still occurs in the case in question (weight equal to 2950 kg), resulting in a calculation error. Specifically, a positive peak is noted in the voltage of the battery pack, accompanied by a negative peak in the pack current (corresponding to the current absorbed by the battery pack itself). These two variables lead to a negative peak in the battery power (representing the power absorbed by the pack), all resulting in the battery SOC (State of Charge) trend as reported in Figure 9 (see in particular the increase in the SOC in the area around 1000 s). All this therefore shows the problem of acquisition errors, which can be incurred by adopting an acquired speed profile instead of a standard one. However, this acquisition inaccuracy and the resolution of this tool calculation error are not of vital importance for the study in question since what is important is the trend of the average consumption over the real driving cycle as the weight of the vehicle varies and not the individual consumption relative to each weight considered.

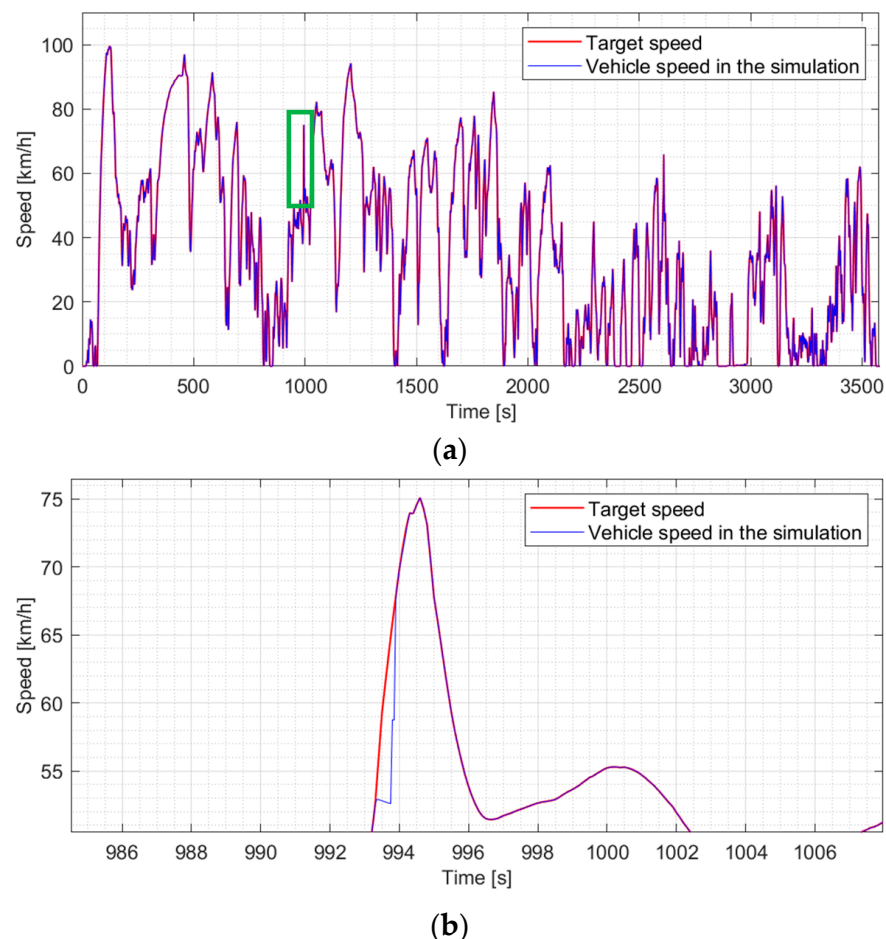


Figure 7. Target speed and vehicle speed in the simulation vs. time elapsed since the beginning of the simulation itself for the N1 vehicle without moments of inertia and with a weight of 2950 kg: (a) for the entire simulation; (b) an enlargement relative to the green box in Figure 7a.

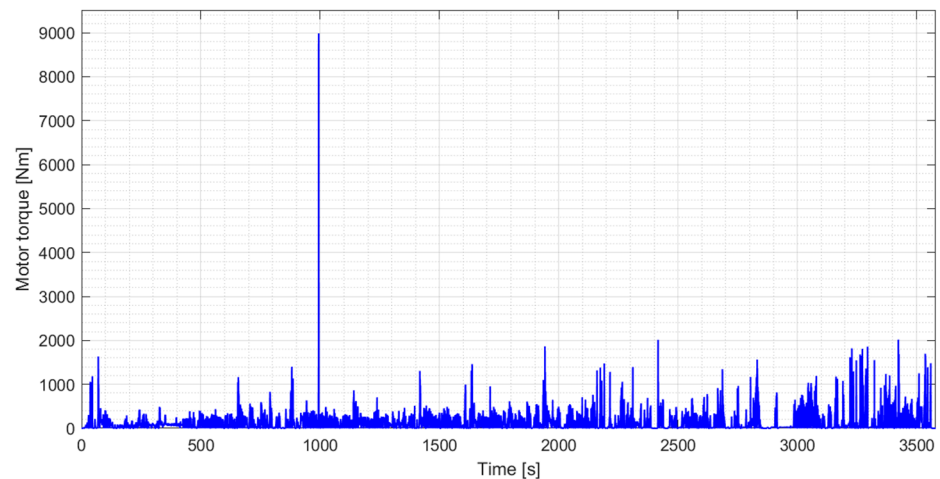


Figure 8. Motor torque vs. time elapsed since the beginning of the simulation for the N1 vehicle without moments of inertia and with a weight of 2950 kg.

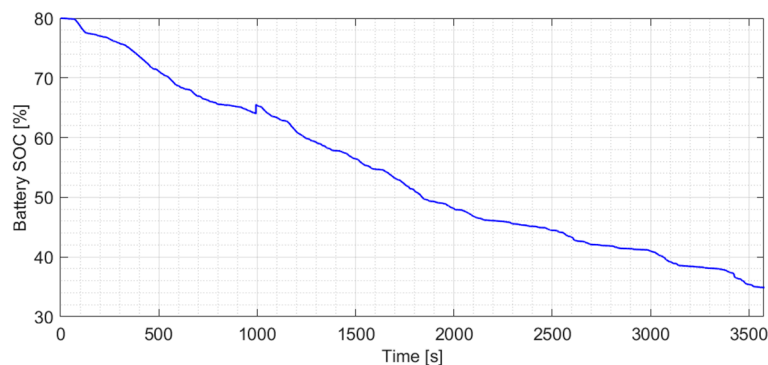


Figure 9. Battery SOC (State of Charge) vs. time elapsed since the beginning of the simulation for the N1 vehicle without moments of inertia and with a weight of 2950 kg.

From the graph in Figure 8, in addition to the peak due to acquisition errors, other peaks are found on about 2000 Nm of torque (unrealistic), but they are only punctual values due to the fact that the speed profile acquired is noisy and can therefore lead to an excessive torque request. Being only punctual values, these affect the results only in a negligible way. The trend line given by the average consumption values over the cycle is in fact still detectable (see Figure 6).

Figure 10 shows the average energy consumption for the sets of simulations for the compact car and N1 models, compared with those of the compact car model with some N1 parameters, relating to the battery pack, the aerodynamics, the transmission efficiency, the rolling resistance, and all the above features simultaneously.

From Figure 10, it is possible to see that the contribution that has the greatest impact on consumption is aerodynamics, followed by the rolling resistance, transmission efficiency, and battery pack. In particular, the last contribution can be considered negligible, especially for simulations with a lower vehicle weight, under 1500 kg approximately. Once again, the same considerations were obtained, which are also valid for the standard driving cycles [28], i.e., for the construction of a vehicle model useful for analyzing the lightweighting, and in particular the average consumption over the considered cycle as the vehicle mass varies. And the most important parameters, to be estimated more precisely, are the aerodynamic contribution, the rolling resistance, and the transmission efficiency.

Furthermore, even for the real driving cycle, as for the standards, the modification of the rolling resistance coefficient involves a greater variation in the slope of the average cycle consumption curve as a function of the vehicle weight, while the modification of the aerodynamics, as we will see better below, involves a less influential variation to this

slope. So, if the objective is to calculate the ERV index, it may be more useful to estimate the resistance to rolling more accurately than the aerodynamic coefficients. In fact, the ERV index represents the slope of the line that interpolates the average consumption as the weight varies. In essence, defining for the compact car (M1) an aerodynamic resistance equal to that of the N1 vehicle leads to an upwards translation of the average consumption curve, whilst it does not lead to a variation in the slope of this curve (and therefore of the ERV index).

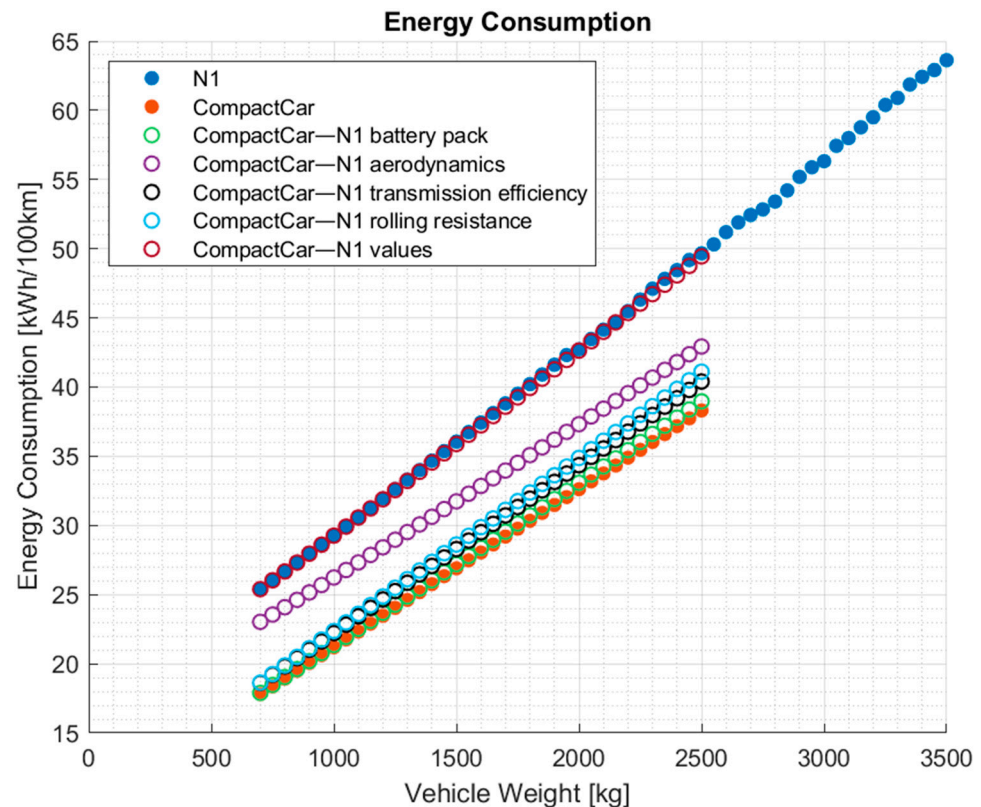


Figure 10. Average energy consumption over the reference real driving cycle, as a function of vehicle weight, for the following vehicle models: the N1 vehicle (“N1”); compact car (“CompactCar”); compact car with the N1 battery pack on board (“CompactCar—N1 battery pack”); compact car with the aerodynamic coefficients of the N1 vehicle (“CompactCar—N1 aerodynamics”); compact car with the transmission efficiency equal to that of the N1 vehicle (“CompactCar—N1 transmission efficiency”); compact car with the rolling resistance coefficient equal to that of the N1 vehicle (“CompactCar—N1 rolling resistance”); and, finally, compact car with all the parameters previously mentioned equal to those of the N1 vehicle (“CompactCar—N1 values”).

In the graph shown in Figure 10, the curve corresponding to the compact car with the battery pack, aerodynamics, transmission efficiency, and rolling resistance parameters identical to those of the N1 vehicle closely aligns with the N1 vehicle’s curve for low vehicle weights. However, at higher weights, torque limitations come into play, causing minor deviations from the target driving cycle in certain small areas, with a consequent slight drop in consumption.

Figure 11 shows the analysis of further parameters, i.e., the inertia contributions and the transmission ratio, including the wheel radius, which contributes to varying the total transmission ratio from the motor to the ground (at the ground contact point of the driving wheels).

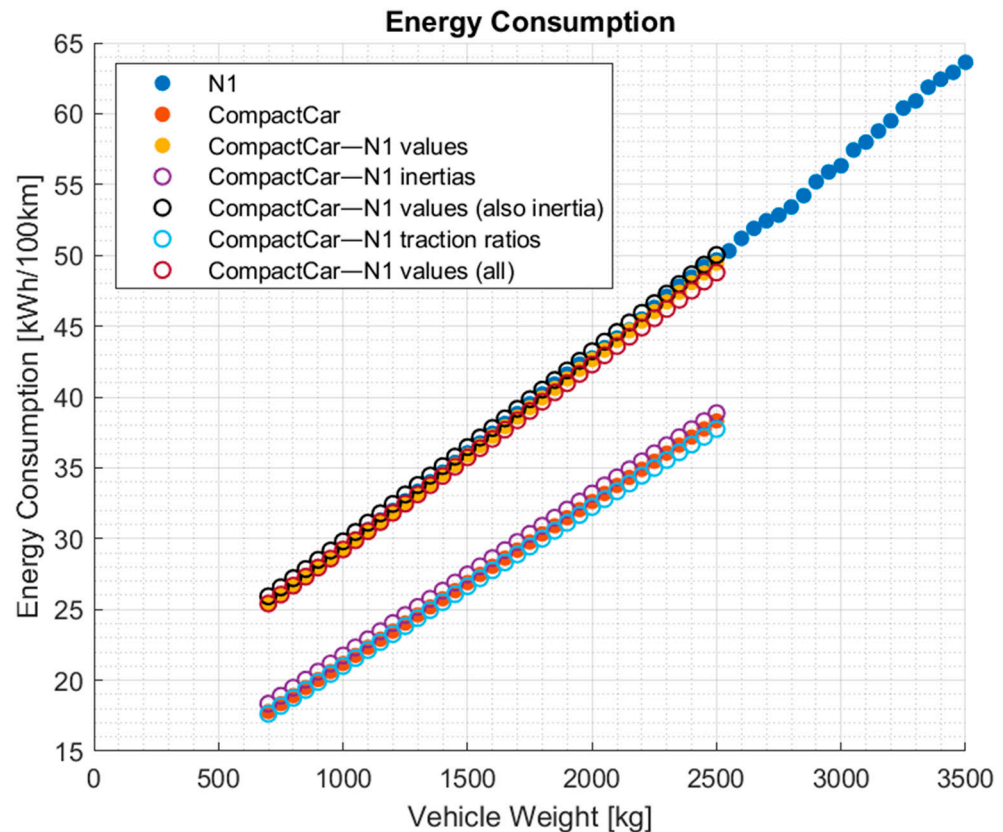


Figure 11. Average energy consumption over the reference real driving cycle, as a function of vehicle weight, for the following vehicle models: the vehicle of category N1 (“N1”); compact car (“CompactCar”); compact car with the battery pack of the N1 vehicle on board, with the aerodynamic coefficients, the efficiency of the transmission, and the rolling resistance coefficient of the N1 vehicle (“CompactCar—N1 values”); compact car with the same moments of inertia as vehicle N1 (“CompactCar—N1 inertias”); compact car with the battery pack, aerodynamics, transmission efficiency, rolling resistance, and moments of inertia of the N1 vehicle (“CompactCar—N1 values (also inertia)”); compact car with the transmission ratios and wheel radii of the N1 vehicle (“CompactCar—N1 traction ratios”); and, finally, compact car with all the previously mentioned parameters equal to those of the N1 vehicle, i.e., the parameters relating to the battery pack, aerodynamics, transmission efficiency, rolling resistance, moments of inertia, transmission ratios, and wheel radii (“CompactCar—N1 values (all)”).

As can be observed from Figure 11, simulating the compact car, but with inertia contributions equal to those of the N1 category vehicle, no particular differences in the results are found. The consumption is approximately the same as the compact car model without modifications. The same thing happens when simulating the compact car model but with transmission ratios and wheel radii equal to those of the N1 vehicle. Instead, using the compact car model with battery pack, aerodynamics, transmission efficiency, and rolling resistance parameters identical to those of the N1 vehicle, no particular differences are obtained by adding the inertia contributions of the N1 and not even considering the total transmission ratios of the N1 vehicle. Therefore, it is sufficient to modify the battery pack, aerodynamics, transmission efficiency, and rolling resistance parameters to modify the compact car model into a model that simulates the behavior of an N1 category vehicle.

This is because inertia, as previously defined, is negligible, and the total transmission ratios (and wheel radii) do not influence the regenerative braking recovery, which is absent (for more details, see [28]). In this case, the transmission ratios only affect the contribution of inertia. If the inertia contributions are zero, a change in the transmission ratio does not lead to a change in consumption, as can be observed in Figure 12 for low vehicle weights.

However, the average consumption with different transmission ratios differs for higher weights. This is most likely due to the difficulty of the heavy vehicle to faithfully follow the imposed real driving cycle, which is “dirtier” than a standard one and characterized by phases of greater acceleration.

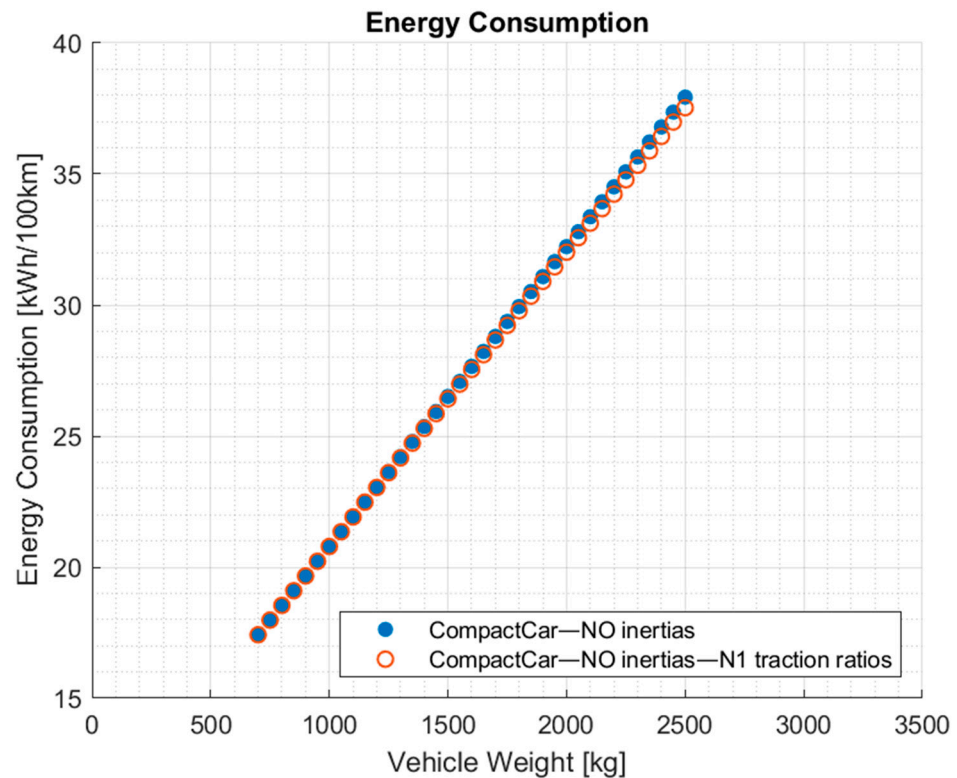


Figure 12. Average energy consumption over the reference real driving cycle, according to the vehicle weight, for the following vehicle models: compact car without inertia (“CompactCar—NO inertias”); compact car with transmission ratios (and wheel radii) equal to those of the N1 vehicle and without inertia (“CompactCar—NO inertias—N1 traction ratios”).

Unless there are limitations for high vehicle weights, the considerations obtained in this section are the same as those obtained for the WLTC (class 3b) and US06 standard cycles in study [28].

3.2. Polynomial Interpolation and ERV Index

In this section, we will examine the polynomial functions that best represent the curves previously shown in Section 3.1. Specifically, the first-, second-, and third-degree polynomial functions were analyzed to approximate the selected curve, with the parameters obtained using “polyfit” function of MATLAB (version R2020b). The function used for polynomial interpolation is presented in Equation (1) of [28] and below in Equation (1).

$$y = c_3 \cdot x^3 + c_2 \cdot x^2 + c_1 \cdot x + c_0 \quad (1)$$

Here, y represents the average energy consumption in kWh/100 km, for the curve analyzed, and x refers to the vehicle weight (in 100 kg). The coefficients c_3 , c_2 , c_1 , and c_0 are the polynomial coefficients determined by the MATLAB “polyfit” function.

Figure 13 shows the curves, relating, respectively, to the N1 vehicle and the compact car, obtained by means of the polynomial functions.

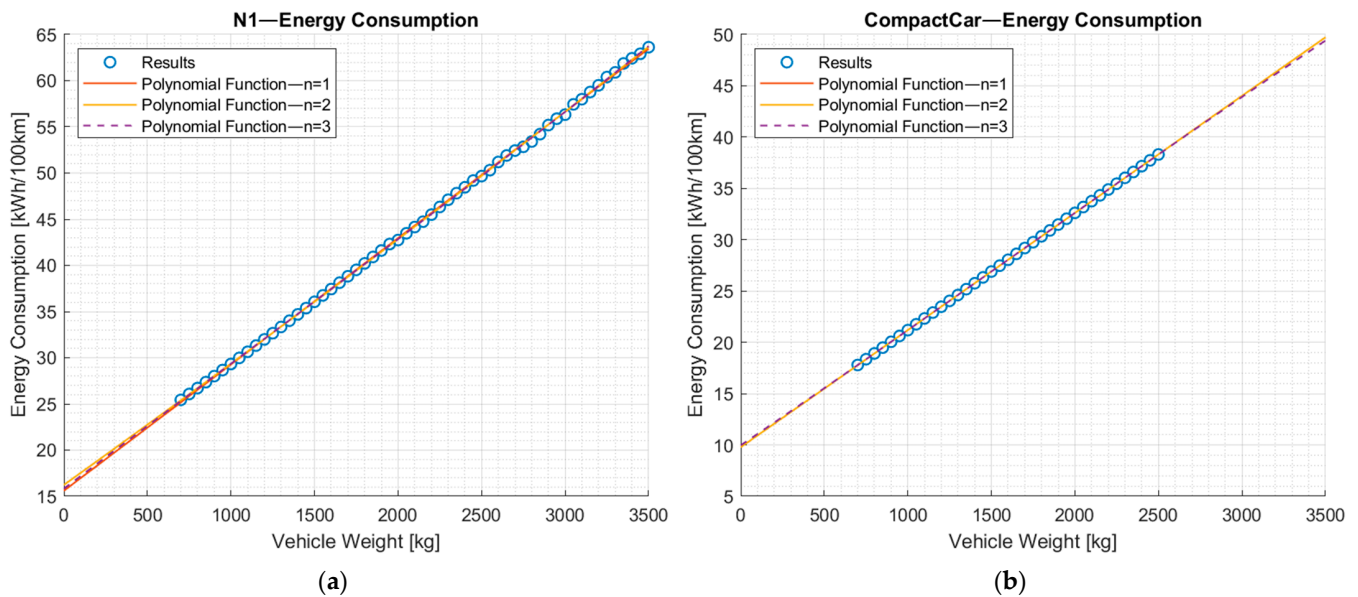


Figure 13. Average energy consumption over reference real driving cycle as a function of the vehicle weight. The curves relating to the results were obtained by means of the simulations (“Results”), and the curves were obtained thanks to the polynomial approximation of the first (“n = 1”), second (“n = 2”), and third degree (“n = 3”) for (a) the N1 vehicle and (b) the compact car.

As can be observed in Figure 13, all three polynomial functions (first, second, and third degree) approximate the represented curves very well. For their description, it is therefore sufficient to approximate with the first-degree polynomial, for greater simplicity. The same result was also observed in all the other simulations conducted (with altered parameters).

Table 3 presents the values of the polynomial coefficients that approximate the consumption–weight curves, with the coefficients obtained using MATLAB’s “polyfit” function. Only the coefficients for the first-degree polynomials are reported, as the second- and third-degree polynomials have negligible c_2 and c_3 coefficients, which are several orders of magnitude smaller than the other two coefficients (c_0 and c_1). In fact, as shown in Figure 13, the curve under consideration can be approximated with sufficient accuracy using only a first-degree polynomial, and the same situation applies to the polynomials corresponding to the curves from all the previous simulations conducted.

Table 3. Coefficients of the polynomial functions that approximate the consumption curves, as a function of the vehicle weight, obtained by means of the simulations on the various vehicle models.

Vehicle Model	Model Description	c_1 [$\frac{\text{kWh}}{100 \text{ km} \cdot 100 \text{ kg}}$]	c_0 [$\frac{\text{kWh}}{100 \text{ km}}$]
N1	N1 model	1.368	15.592
N1— NO inertias	N1 model without inertia contributions	1.365	15.201
CompactCar	Compact car model	1.141	9.782
CompactCar— NO inertias	Compact car model without inertia contributions	1.141	9.406
CompactCar— N1 battery pack	Compact car model with the N1 battery pack on board	1.172	9.633
CompactCar— N1 aerodynamics	Compact car model with the aerodynamic coefficients of the N1 vehicle	1.109	15.149
CompactCar— N1 transmission efficiency	Compact car model with the transmission efficiency equal to that of the N1 vehicle	1.211	10.110

Table 3. Cont.

Vehicle Model	Model Description	c_1 [$\frac{\text{kWh}}{100 \text{ km} \cdot 100 \text{ kg}}$]	c_0 [$\frac{\text{kWh}}{100 \text{ km}}$]
CompactCar— N1 rolling resistance	Compact car model with the rolling resistance coefficient equal to that of the N1 vehicle	1.250	9.875
CompactCar— N1 values	Compact car model compact car with all the above-mentioned parameters equal to those of the N1 vehicle	1.339	15.862
CompactCar— N1 inertias	Compact car model with the same moments of inertia as vehicle N1	1.141	10.345
CompactCar— N1 values (also inertia)	Compact car model compact car with all the above-mentioned parameters (also moments of inertia) equal to those of the N1 vehicle	1.342	16.385
CompactCar— N1 traction ratios	Compact car model with the transmission ratios and wheel radii of the N1 vehicle	1.119	9.832
CompactCar— N1 inertias and traction ratios	Compact car model with the moments of inertia, the transmission ratios and wheel radii of the N1 vehicle	1.118	10.031
CompactCar— N1 values (all)	Compact car model compact car with all the above-mentioned parameters equal to those of the N1 vehicle, including the moments of inertia, traction ratios, and wheel radii	1.303	16.209

As mentioned in the Introduction Section (Section 1), the FRV index is often referenced in the literature when calculating the energy savings associated with vehicle lightweighting. For electric vehicles, however, it is more appropriate to calculate an equivalent index, the ERV index, which corresponds to the c_1 coefficient of the first-degree polynomial, presented in Table 3 for each simulated vehicle model.

Figure 14 reports the ERV index, calculated for each pair of average consumptions over the reference real driving cycle, for consecutive weights; for further information, refer to Equation (2) of [28].

From Figure 14a, it can be seen that the technique consisting of obtaining the ERV index point by point is not effective for high vehicle weights. This is due to the limitations that arise when the vehicle is not equipped with sufficient performance in order to follow the acceleration targets. This phenomenon was not observed in [28] for the WLTC and US06 standardized cycles; in fact, the standard driving cycles are usually characterized by low accelerations, which are not very realistic. The real driving cycles, unlike the standardized ones, due to speed profile acquisition errors, are therefore able to cause a crisis in the simulation tools, thus making them more difficult to manage.

For low vehicle weights, Figure 14b highlights some previous aspects, such as the minimal influence of inertia on consumption variation, making the inertia negligible in the context of this study, which aims to assess the effects of vehicle lightweighting. Moreover, for the same vehicle model, the ERV index increases as the vehicle weight increases. This indicates that heavier vehicles benefit more from lightweighting for the same weight reduction. Additionally, it is possible to observe which parameters (when equal to those of a higher-class vehicle, such as class N1 in this case) raise the ERV index and which lower it. For example, it can be observed that the rolling resistance has a major influence on the ERV index, i.e., on the slope of the average energy consumption curve as a function of weight.

To estimate the reduction in the average consumption over real driving cycles following the vehicle lightweighting, it is therefore more appropriate to obtain the ERV index as the c_1 coefficient of the first-degree polynomial function that approximates the average consumption curve identified by means of simulations. In this way, for each vehicle, the ERV index is approximated to a single constant value independent of the vehicle weight. However, this approximation is reasonable, as can be observed in Figure 14b, especially for the compact car.

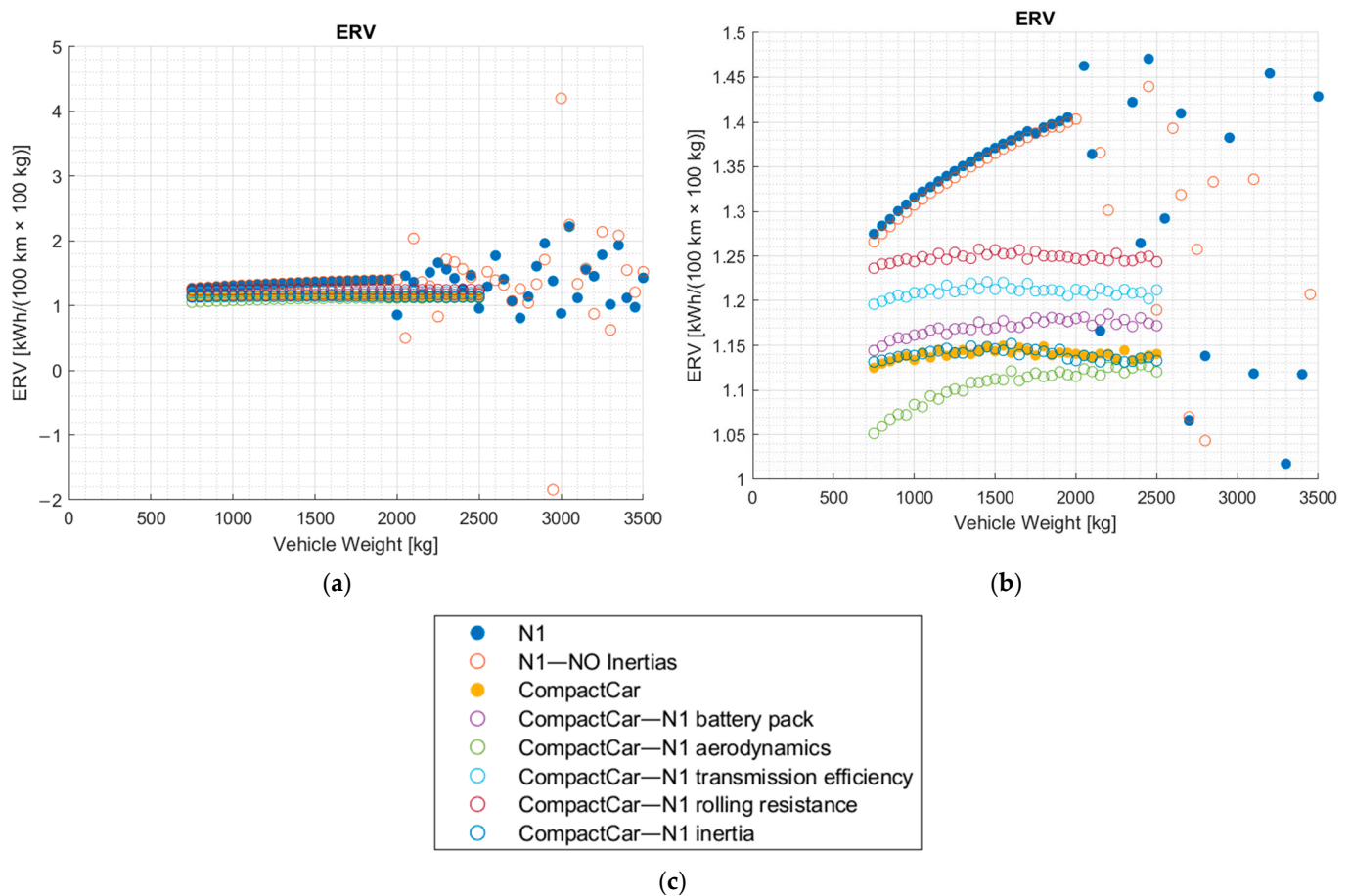


Figure 14. ERV index, calculated for the reference real driving cycle and calculated between a simulation performed at a given vehicle weight and the simulation with the vehicle weight immediately lower than that under examination (considering the set of simulations performed), as a function of the vehicle weight, for the following vehicle models: the N1 category vehicle (“N1”); N1 vehicle with zero inertia (“N1—NO Inertias”); compact car (“CompactCar”); compact car with the N1 battery pack on board (“CompactCar—N1 battery pack”); compact car with the aerodynamic coefficients of the N1 vehicle (“CompactCar—N1 aerodynamics”); compact car with the transmission efficiency equal to that of the N1 vehicle (“CompactCar—N1 transmission efficiency”); compact car with the N1 vehicle rolling resistance coefficient (“CompactCar—N1 rolling resistance”); and, finally, compact car with moments of inertia equal to those of the N1 vehicle (“CompactCar—N1 inertia”). In particular, in (a), the graph with all the ERV indexes calculated; in (b), the graph with the y -axis limited between 1 and 1.5 kWh/(100 km·100 kg); and in (c), the legend valid for both graphs.

Now, for each compact car weight, starting from the same vehicle but with an additional 300 kg of weight, the ERV index obtained from the polynomial function is used to determine the average consumption over the reference driving cycle. Furthermore, multiple ERV indices are assumed, reported in Table 3, obtained by assuming errors in the construction of the model, in particular by mistakenly setting one or more parameters equal to those of the N1 category vehicle. The result of these tests is reported in Figure 15.

Figure 15 shows that an incorrect definition of the model does not cause significant errors in the evaluation of a 300 kg weight reduction, as long as the vehicle’s actual consumption in the given real driving cycle is known, as obtained in [28] for the WLTP and US06 standard cycles. This approach reveals a contrasting situation compared to evaluating lightweighting based on the consumption curve obtained through vehicle model simulations. In the latter case, as shown in Figure 10, an incorrect assessment of the vehicle model parameters, in particular relating to the aerodynamics, can cause a non-negligible

error. In fact, increasing the aerodynamic resistance coefficient, as seen in Figure 10, raises the consumption curve, but it has little effect on the slope of the curve itself.

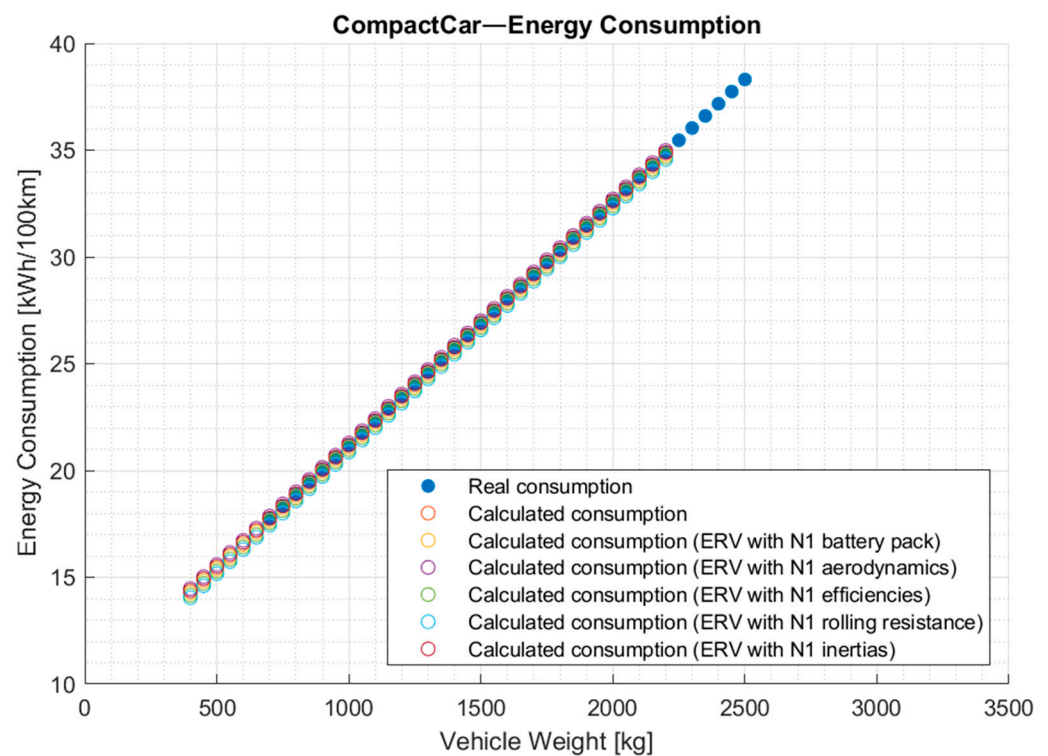


Figure 15. Average energy consumption over the reference real driving cycle, as a function of vehicle weight, for the compact car, obtained through simulations with the TEST model (“Real consumption”) and considering the ERV obtained through polynomial interpolation, for the following vehicle models (lightweighting by 300 kg): CompactCar (“Calculated consumption”); CompactCar with the vehicle battery pack N1 on board (“Calculated consumption (ERV with N1 battery pack)”); CompactCar with the aerodynamic coefficients of vehicle N1 (“Calculated consumption (ERV with the N1 aerodynamics)”); CompactCar with the transmission efficiency equal to that of the N1 vehicle (“Calculated consumption (ERV with N1 efficiencies)”); CompactCar with the vehicle rolling resistance coefficient of N1 (“Calculated consumption (ERV with N1 rolling resistance)”); and, finally, CompactCar with the moments of inertia of vehicle N1 (“Calculated consumption (ERV with N1 inertias)”).

Therefore, if the consumption data for the reference cycle are available and we want to assess the results of a hypothetical lightweighting, it is more convenient to use the constant ERV index approach (polynomial interpolation) for more realistic conclusions. The same consideration has also been deduced for the standard driving cycles analyzed in [28].

3.3. Comparison Between the Reference Real-World Driving Cycle and Standard Cycles

In this section, the consumption curves obtained for the real reference driving cycle are compared with the curves obtained for different standardized cycles [28]. This has the ultimate aim of evaluating which standard driving cycle can be most representative of the real case under examination and which of these can therefore be useful for estimating the impact of vehicle lightweighting for the case of northern Italy.

Figure 16 shows the average energy consumption obtained from various sets of simulations across the reference real driving cycle and different regulated cycles [28]. Specifically, each point on the graph represents the average energy consumption over the analyzed cycle, determined by running a simulation with the TEST model on the respective cycle, with a pre-set weight (as indicated on the x -axis of the graph).

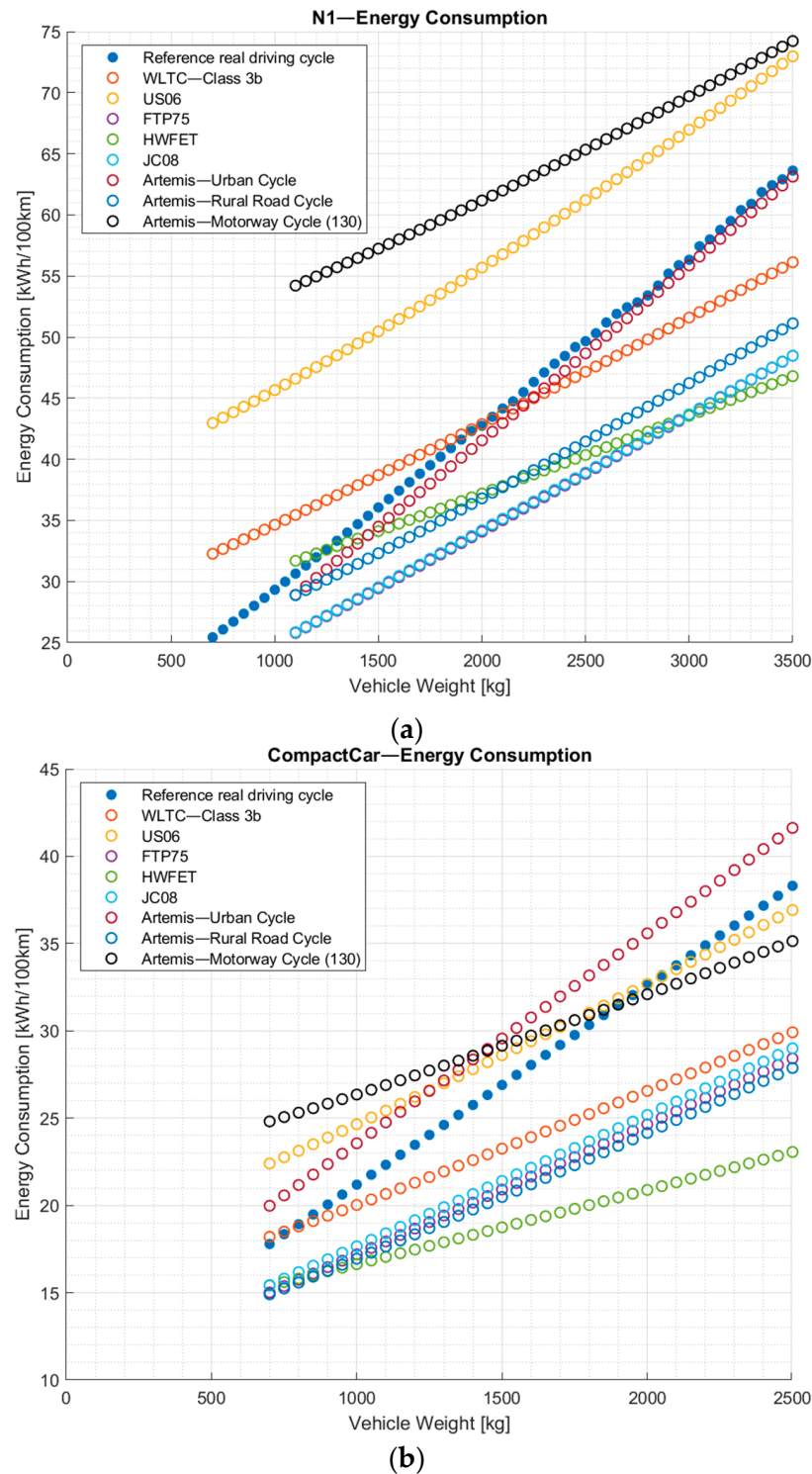


Figure 16. Average energy consumption, for (a) the N1 category vehicle and (b) compact car, over the reference real driving cycle and the following standard driving cycles: WLTC (class 3b); US06; FTP75; HWFET; JC08; Artemis Urban Cycles; Artemis Rural Road Cycle; and Artemis Motorway Cycle (130) [28].

From Figure 16a, it can be observed that, for light commercial vehicles (category N1), the standard driving cycle that best represents the real case object of this study is the Artemis Urban Cycle. It should be remembered that the real driving cycle considered is representative of home–work trips, from the province of Brescia, crossing the city of Brescia, in the Lombardy region, in northern Italy.

For the compact vehicle, however, there is no standardized driving cycle that accurately approximates the real reference driving cycle. However, it can be noted that the slope of the consumption curve calculated for the real cycle is quite close to the slope of the curve obtained for the Artemis Urban Cycle. It follows that this last cycle can be useful for estimating the outcome of the lightweighting also for compact cars, provided that only the ERV index is considered.

The similarity between the ERV indices for the Artemis Urban Cycle speed profile and those obtained for the real driving cycle can also be observed in Table 4 (for N1 category vehicle) and in Table 5 (for compact car). It is worth noting that the ERV index corresponds to the c_1 coefficient of the first-degree polynomial function.

Table 4. Coefficients of the polynomial functions (first degree), which approximate the consumption curves as a function of the vehicle weight obtained by means of simulations on the N1 category vehicle model, for the reference real driving cycle and for the following standard driving cycles: WLTC (class 3b); US06; FTP75; HWFET; JC08; Artemis Urban Cycles; Artemis Rural Road Cycle; and Artemis Motorway Cycle (130) [28].

Driving Cycle	c_1 $\left[\frac{\text{kWh}}{100 \text{ km} \cdot 100 \text{ kg}} \right]$	c_0 $\left[\frac{\text{kWh}}{100 \text{ km}} \right]$
Reference real driving cycle	1.368	15.592
WLTC—Class 3b	0.852	25.995
US06	1.077	34.562
FTP75	0.946	15.229
HWFET	0.630	24.647
JC08	0.944	15.362
Artemis—Urban Cycle	1.426	13.082
Artemis—Rural Road Cycle	0.929	18.344
Artemis—Motorway Cycle (130)	0.835	44.654

Table 5. Coefficients of the polynomial functions (first degree), which approximate the consumption curves as a function of the vehicle weight obtained by means of simulations on the compact car model, for the reference real driving cycle and for the following standard driving cycles: WLTC (class 3b); US06; FTP75; HWFET; JC08; Artemis Urban Cycles; Artemis Rural Road Cycle; and Artemis Motorway Cycle (130) [28].

Driving Cycle	c_1 $\left[\frac{\text{kWh}}{100 \text{ km} \cdot 100 \text{ kg}} \right]$	c_0 $\left[\frac{\text{kWh}}{100 \text{ km}} \right]$
Reference real driving cycle	1.141	9.782
WLTC—Class 3b	0.654	13.488
US06	0.809	16.549
FTP75	0.746	9.742
HWFET	0.426	12.370
JC08	0.754	10.114
Artemis—Urban Cycle	1.203	11.528
Artemis—Rural Road Cycle	0.723	9.709
Artemis—Motorway Cycle (130)	0.482	21.253

Finally, Figure 16 illustrates how variations in vehicle weight can cause a standard driving cycle to either underestimate or overestimate energy consumption. For instance,

for the N1 category vehicle, for the considered home–work travel, the WLTC driving cycle underestimates real consumption when the vehicle weight is below approximately 2100 kg. Conversely, for higher weights, it overestimates consumption.

4. Discussion

In this paper, the outcome of vehicle lightweighting on a real-world driving cycle was analyzed, emphasizing the identification of vehicle model parameters that most significantly influence the results. Consequently, it highlights which parameters require more precise estimation for an accurate analysis. In particular, one objective is to compare the results obtained for the real-world cycle with those obtained in [28] using the WLTC (class 3b) and US06 standard driving cycles.

As seen in [28] for the two standard cycles, the contribution of the moments of inertia on energy consumption can also be considered negligible for the real cycle, for both the N1 category vehicle and compact car. Instead, the aspect that has the greatest impact on higher consumption is the increase in aerodynamic resistance, followed by rolling resistance, while the aspect that least affects consumption is the battery pack, followed by the efficiency of the transmission.

In particular, the increase in aerodynamic drag has a significant impact on the absolute value of the average vehicle consumption on the real cycle; however, it does not lead to a notable change in the slope of the consumption curve, as observed in [28] for the two normed cycles.

Finally, to estimate the vehicle consumption accurately and therefore to effectively evaluate the outcome of the lightweighting, it may be sufficient to correctly set the vehicle model parameters relating to the battery pack, aerodynamics, transmission efficiency, and rolling resistance, as stated in [28]. Meanwhile, regarding the functions that approximate the consumption curves identified through simulations, it is enough to consider the first-degree polynomial functions for a good level of precision.

The ERV index, useful for analyzing the lightweighting results for electric vehicles, expressed in kWh/(100 km·100 kg), increases as the vehicle weight rises for the same vehicle model. This implies that heavier vehicles benefit more from lightweighting for the same amount of weight reduction. The vehicle parameters that most influence the ERV index are the transmission efficiency and those relating to the battery pack. Aerodynamics, on the other hand, has little influence since it modifies consumption in a non-negligible way but not the slope of the average consumption curve as a function of vehicle weight. This therefore applies to the reference real-world driving cycle considered in this study, as seen in [28] for the WLTC (class 3b) and US06 standard cycles.

Figure 17 summarizes the ERV indices obtained for the reference real-world driving cycle for the different vehicle models.

Then, the results obtained for the real-world driving cycle, in terms of consumption as the vehicle weight varies, were compared with the results obtained in [28] for different standard driving cycles: WLTC (class 3b); US06; FTP75; HWFET; JC08; and Artemis Urban, Rural Road, and Motorway cycles.

From this comparison it has been found that, for light commercial vehicles (N1 category), the standard driving cycle that best fits the home-to-work journey in the reference geographic area considered is the Artemis Urban Cycle. In fact, the curve of the average consumption for the cycle as a function of the vehicle weight matches well between the real-world cycle and the Artemis Urban Cycle.

This standardized cycle can also be considered useful for estimating the lightweighting result for compact cars. Although the consumption curve obtained for the real cycle does not match that of the Artemis Urban Cycle, the slope of this curve (which is roughly a straight line) is quite similar. Therefore, both the reference real-world driving cycle and the Artemis Urban Cycle share the same ERV index for compact vehicles.

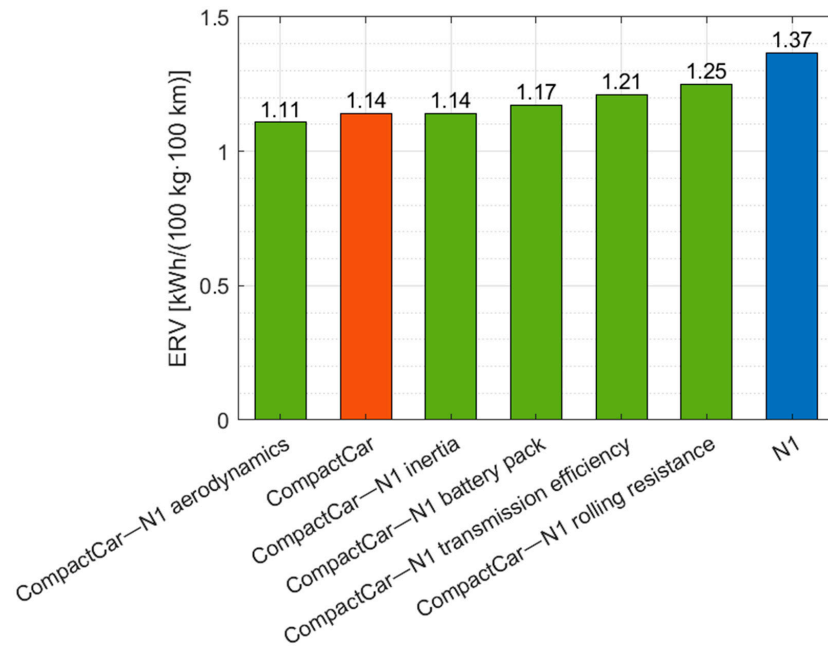


Figure 17. ERV index, obtained from the “polyfit” MATLAB function, for the reference real driving cycle, for the N1 vehicle, for the compact car, and for the compact car, with the following parameters, aspects, and components of the N1 vehicle: aerodynamics; moments of inertia; battery pack; transmission efficiency; and rolling resistance.

Finally, Figure 18 summarizes the impact of vehicle lightweighting across different driving cycles, presenting the ERV indices obtained for each cycle for both the N1 category vehicle and the compact car. From this figure, it is evident that, for the case study in this paper, the most representative standard driving cycle for both vehicles is the Artemis Urban Cycle. In fact, this cycle has ERV indices very similar to those calculated for the real driving cycle.

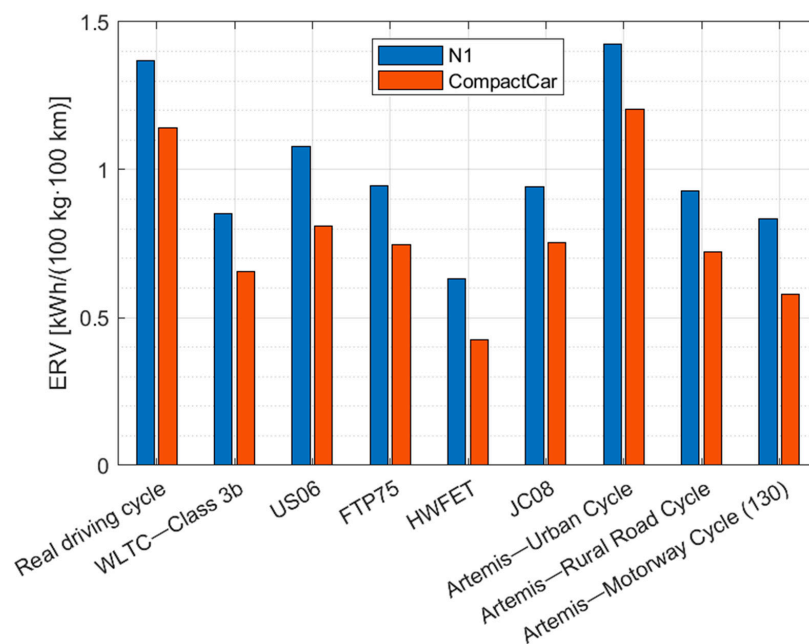


Figure 18. ERV index, obtained from the “polyfit” MATLAB function, for different standard driving cycles, for the N1 vehicle and for the compact car [28].

Furthermore, from Figure 18, it is possible to observe that the real driving cycle and the urban Artemis are those that present the highest ERV index, both for the compact car and for the N1 vehicle. Therefore, they are the two cycles that, among those considered, allow for obtaining the greatest benefits from the vehicle lightweighting process. Conversely, the least benefits are obtained by following the standardized HWFET driving cycle.

5. Conclusions

In this study, the research conducted in [32] was replicated using a real-world driving cycle, recorded via GPS on a vehicle, to represent typical home-to-work commutes in northern Italy, specifically around the city and province of Brescia in Lombardy.

In the fuel efficiency literature, the Fuel Reduction Value (FRV) index, expressed in L/(100 km·100 kg), is commonly used to estimate fuel savings from vehicle lightweighting. For electric vehicles, however, an equivalent index—the Energy Reduction Value (ERV)—expressed in kWh/(100 km·100 kg), is more appropriate, as it directly measures energy savings without converting them to fuel-equivalent liters.

The actual ERV for a given vehicle model generally increases with vehicle weight, meaning that heavier vehicles generally gain greater benefits from the same level of weight reduction. However, assuming a constant ERV across weight variations is a reasonable approximation within the same vehicle model. This holds especially true for the specific real-world driving cycle examined, where consumption patterns for both N1 category vehicles and compact cars, as the weight varies, are well approximated by linear relationships (i.e., first-degree polynomial functions).

In this study, it was observed that for an accurate calculation of the ERV index—even for the selected real-world driving cycle, and consistent with standardized cycles such as the WLTC (class 3b) and US06 cycles analyzed in [32]—it is crucial to accurately define parameters such as the rolling resistance coefficient, aerodynamics, battery pack characteristics, and transmission efficiency, while the impact of inertia can be considered negligible.

The results obtained for the real-world driving cycle, in terms of average energy consumption as a function of the vehicle weight and ERV index, were then compared with those from several standardized cycles: WLTC (class 3b); US06; FTP75; HWFET; JC08; and the Artemis Urban, Rural Road, and Motorway cycles [32]. Among these, the Artemis Urban Cycle was identified as most representative of home-to-work travel from the province of Brescia to the city center. Specifically, for N1 category vehicles, the average consumption for the real cycle closely aligns with the Artemis cycle across all vehicle weights. For compact cars, this alignment holds true only with respect to the ERV index, which, when the base vehicle's consumption is known, serves as a valuable indicator for assessing potential lightweighting outcomes.

This paper, by outlining the methodology for the creation of a lightweighting model—i.e., identifying the parameters to consider for its construction—provides a starting point for analyzing the outcomes of the vehicle lightweighting for other electric vehicles and other driving cycles. These driving cycles can be real or standardized, related to a real driver or using autonomous vehicles [52], but in any case, they must be representative of the geographical region of interest, of the travel time (and the related traffic level), and of the vehicle's mission (for private use, a bus with a predefined mission, an autonomous bus, etc.). This type of study is important because achieving effective lightweighting to reduce consumption can partly mitigate a critical issue of electric vehicles, namely, the limited range of the traction battery, which is also associated with long recharging times. This study was conducted on a real-world driving cycle that represents the home-to-work commute from the province of Brescia to the city, a predominantly urban journey characterized by relatively heavy traffic. This real cycle is therefore specific to the geographical area of both departure and arrival. For other geographical regions, it is necessary to identify a new real-world reference cycle and retrace the methodology outlined in this scientific article.

Another limitation of this study is that the real reference driving cycle was obtained using a traditional internal combustion vehicle due to availability reasons. However, as

stated in [53], in general, a driving cycle performed on the road with an internal combustion vehicle differs from one obtained with an electric vehicle, given the typically higher maximum accelerations of the latter. It will therefore be interesting, in the future, to repeat this work by acquiring further real driving cycles on board electric vehicles.

Future work will focus on building a comprehensive vehicle database across various classes, enabling precise estimation of the parameters that most influence lightweighting outcomes, following the approach outlined here and in [32]. This database would ideally include the ERV index for each vehicle across a set of standardized cycles and, where possible, multiple real-world cycles that represent distinct regions or types of journeys. Additionally, the goal would be to identify the standardized cycle that best corresponds to each real-world cycle.

Author Contributions: Conceptualization, G.S. and D.C.; methodology, G.S.; software, G.S.; formal analysis, G.S., M.G. and D.C.; data curation, G.S., A.C. and P.M.; writing—original draft preparation, G.S.; writing—review and editing, G.S., D.C. and M.G.; visualization, M.G. and D.C.; supervision, M.G. and D.C. All authors have read and agreed to the published version of the manuscript.

Funding: This research is funded by the European Union, NextGenerationEU, see below.

Data Availability Statement: The data presented in this study are available on request from the corresponding author. The data are not publicly available due to the University of Brescia’s privacy policy.

Acknowledgments: This study was financed by the European Union—NextGenerationEU (National Sustainable Mobility Center CN00000023, Italian Ministry of University and Research Decree n. 1033—17/06/2022, Spoke 11—Innovative Materials & Lightweighting). The opinions expressed are those of the authors only and should not be considered as representative of the European Union or the European Commission’s official position. Neither the European Union nor the European Commission can be held responsible for them. CUP D83C22000690001.

Conflicts of Interest: The authors declare no conflicts of interest.

Nomenclature

Abbreviation	Description
Af	Frontal area of the vehicle
c_3, c_2, c_1, c_0	Coefficients of the y polynomial
Cx	Longitudinal aerodynamic coefficient (drag)
DEM	Digital Elevation Model
EPA	U.S. Environmental Protection Agency
ERV	Energy Reduction Value
EV	Electric vehicle
FRV	Fuel Reduction Value
FTP75	Standard driving cycle (FTP75) described in the EPA Federal Test Procedure (FTP)
GPS	Global Position System
HWFET	EPA Highway Fuel Economy Cycle
JC08	Japanese Emission Test Cycle
SFTP	EPA Supplemental Federal Test Procedure
SFTP-US06	Standard driving cycle (US06) described in the EPA Supplemental Federal Test Procedure (SFTP)
TEST	Target-speed EV Simulation Tool
WLTC	Worldwide Harmonized Light-Duty Vehicles Test Cycle
WLTP	Worldwide Harmonized Light-Duty Vehicles Test Procedure
x	Vehicle weight (expressed in 100 kg)
y	Polynomial interpolation function, energy consumption expressed in kWh/(100 km)

References

1. European Council. Council of the European Union Stricter CO₂ Emission Standards for Cars and Vans Signed Off by the Council. Available online: <https://www.consilium.europa.eu/en/press/press-releases/2019/04/15/stricter-co2-emission-standards-for-cars-and-vans-signed-off-by-the-council/> (accessed on 28 October 2024).
2. European Law Brussels, 3 April 2019. PE-CONS 6/19. Regulation of the European Parliament and of the Council Setting CO₂ Emission Performance Standards for New Passenger Cars and for New Light Commercial Vehicles, and Repealing Regulations (EC) No 443/2009 and (EU) No 510/2011 (Recast). Available online: <https://data.consilium.europa.eu/doc/document/PE-6-2019-INIT/en/pdf> (accessed on 30 August 2022).
3. European Parliament and Council of the European Union Ordinary Legislative Procedure 2021/0197(COD). Available online: [https://oeil.secure.europarl.europa.eu/oeil/en/procedure-file?reference=2021/0197\(COD\)](https://oeil.secure.europarl.europa.eu/oeil/en/procedure-file?reference=2021/0197(COD)) (accessed on 8 January 2024).
4. Ehsani, M.; Gao, Y.; Longo, S.; Ebrahimi, K. *Modern Electric, Hybrid Electric, and Fuel Cell Vehicles*; CRC Press, Taylor & Francis Group: Boca Raton, FL, USA, 2018; pp. 1–11.
5. Lewis, G.M.; Buchanan, C.A.; Jhaveri, K.D.; Sullivan, J.L.; Kelly, J.C.; Das, S.; Taub, A.I.; Keoleian, G.A. Green Principles for Vehicle Lightweighting. *Environ. Sci. Technol.* **2019**, *53*, 4063–4077. [[CrossRef](#)] [[PubMed](#)]
6. Spreafico, C. Can Modified Components Make Cars Greener? A Life Cycle Assessment. *J. Clean. Prod.* **2021**, *307*, 127190. [[CrossRef](#)]
7. Koffler, C.; Rohde-Brandenburger, K. On the Calculation of Fuel Savings through Lightweight Design in Automotive Life Cycle Assessments. *Int. J. Life Cycle Assess.* **2010**, *15*, 128–135. [[CrossRef](#)]
8. Delogu, M.; Zanchi, L.; Dattilo, C.A.; Pierini, M. Innovative Composites and Hybrid Materials for Electric Vehicles Lightweight Design in a Sustainability Perspective. *Mater. Today Commun.* **2017**, *13*, 192–209. [[CrossRef](#)]
9. MacKenzie, D.; Zoepf, S.; Heywood, J. Determinants of US Passenger Car Weight. *Int. J. Veh. Des.* **2014**, *65*, 73–93. [[CrossRef](#)]
10. Kim, H.C.; Wallington, T.J. Life-Cycle Energy and Greenhouse Gas Emission Benefits of Lightweighting in Automobiles: Review and Harmonization. *Environ. Sci. Technol.* **2013**, *47*, 6089–6097. [[CrossRef](#)]
11. Helms, H.; Lambrecht, U. The Potential Contribution of Light-Weighting to Reduce Transport Energy Consumption. *Int. J. Life Cycle Assess.* **2007**, *12*, 58–64.
12. Candela, A.; Sandrini, G.; Gadola, M.; Chindamo, D.; Magri, P. Lightweighting in the Automotive Industry as a Measure for Energy Efficiency: Review of the Main Materials and Methods. *Heliyon* **2024**, *10*, e29728. [[CrossRef](#)]
13. Cheah, L.; Heywood, J. Meeting U.S. Passenger Vehicle Fuel Economy Standards in 2016 and Beyond. *Energy Policy* **2011**, *39*, 454–466. [[CrossRef](#)]
14. Caffrey, C.; Bolon, K.; Kolwich, G.; Johnston, R.; Shaw, T. *Cost-Effectiveness of a Lightweight Design for 2020–2025: An Assessment of a Light-Duty Pickup Truck*; SAE Technical Paper: Warrendale, PA, USA, 2015. [[CrossRef](#)]
15. Kollamthodi, S.; Kay, D.; Skinner, I.; Dun, C.; Hausberger, S. The Potential for Mass Reduction of Passenger Cars and Light Commercial Vehicles in Relation to Future CO₂ Regulatory Requirements. Available online: https://climate.ec.europa.eu/system/files/2016-11/ldv_downweighting_co2_report_en.pdf (accessed on 14 November 2022).
16. Lutsey, N. Review of Technical Literature and Trends Related to Automobile Mass-Reduction Technology. In *Institute of Transportation Studies*; University of California, Davis: Davis, CA, USA, 2010; Volume UCD-ITS-RR-10-10, pp. 1–40.
17. Giordano, G. Plastics Power a New Generation of Electric Vehicles. *Plast. Eng.* **2019**, *75*, 24–33. [[CrossRef](#)]
18. Zecchi, L.; Sandrini, G.; Gadola, M.; Chindamo, D. Modeling of a Hybrid Fuel Cell Powertrain with Power Split Logic for Onboard Energy Management Using a Longitudinal Dynamics Simulation Tool. *Energies* **2022**, *15*, 6228. [[CrossRef](#)]
19. Sandrini, G.; Gadola, M.; Chindamo, D.; Zecchi, L. Model of a Hybrid Electric Vehicle Equipped with Solid Oxide Fuel Cells Powered by Biomethane. *Energies* **2023**, *16*, 4918. [[CrossRef](#)]
20. Osborne, J. FEATURE: Light Speed—How Electric Cars Are Driving a New Wave of Lightweighting. Institution of Mechanical Engineers. Available online: <https://www.imeche.org/news/news-article/feature-light-speed-how-electric-cars-are-driving-a-new-wave-of-lightweighting> (accessed on 14 November 2022).
21. Sandrini, G.; Gadola, M.; Chindamo, D.; Magri, P. Efficient Regenerative Braking Strategy Aimed at Preserving Vehicle Stability by Preventing Wheel Locking. *Transp. Res. Procedia* **2023**, *70*, 28–35. [[CrossRef](#)]
22. Sandrini, G.; Chindamo, D.; Gadola, M.; Candela, A.; Magri, P. Primary and Secondary Vehicle Lightweighting Achieved by Acting on the Battery Thermal Management System. In *AVEC 2024, LNME*; Mastinu, G., Braghin, F., Cheli, F., Corno, M., Savaresi, S.M., Eds.; Springer: Berlin/Heidelberg, Germany, 2024; pp. 308–314.
23. Kim, H.C.; Wallington, T.J.; Sullivan, J.L.; Keoleian, G.A. Life Cycle Assessment of Vehicle Lightweighting: Novel Mathematical Methods to Estimate Use-Phase Fuel Consumption. *Environ. Sci. Technol.* **2015**, *49*, 10209–10216. [[CrossRef](#)]
24. Del Pero, F.; Delogu, M.; Pierini, M. The Effect of Lightweighting in Automotive LCA Perspective: Estimation of Mass-Induced Fuel Consumption Reduction for Gasoline Turbocharged Vehicles. *J. Clean. Prod.* **2017**, *154*, 566–577. [[CrossRef](#)]
25. Delogu, M.; Del Pero, F.; Pierini, M. Lightweight Design Solutions in the Automotive Field: Environmental Modelling Based on Fuel Reduction Value Applied to Diesel Turbocharged Vehicles. *Sustainability* **2016**, *8*, 1167. [[CrossRef](#)]
26. Kim, H.C.; Wallington, T.J. Life Cycle Assessment of Vehicle Lightweighting: A Physics-Based Model To Estimate Use-Phase Fuel Consumption of Electrified Vehicles. *Environ. Sci. Technol.* **2016**, *50*, 11226–11233. [[CrossRef](#)] [[PubMed](#)]
27. Del Pero, F.; Berzi, L.; Antonacci, A.; Delogu, M. Automotive Lightweight Design: Simulation Modeling of Mass-Related Consumption for Electric Vehicles. *Machines* **2020**, *8*, 51. [[CrossRef](#)]

28. Sandrini, G.; Gadola, M.; Chindamo, D.; Candela, A.; Magri, P. Exploring the Impact of Vehicle Lightweighting in Terms of Energy Consumption: Analysis and Simulation. *Energies* **2023**, *16*, 5157. [CrossRef]
29. Del Pero, F.; Delogu, M.; Berzi, L.; Dattilo, C.A.; Zonfrillo, G.; Pierini, M. Sustainability Assessment for Different Design Solutions within the Automotive Field. *Procedia Struct. Integr.* **2019**, *24*, 906–925. [CrossRef]
30. Quirama, L.F.; Giraldo, M.; Huertas, J.I.; Tibaquirá, J.E.; Cordero-Moreno, D. Main Characteristic Parameters to Describe Driving Patterns and Construct Driving Cycles. *Transp. Res. D Transp. Environ.* **2021**, *97*, 102959. [CrossRef]
31. Puchalski, A.; Komorska, I. Stochastic Simulation and Validation of Markov Models of Real Driving Cycles. *Diagnostyka* **2019**, *20*, 31–36. [CrossRef]
32. Ma, R.; He, X.; Zheng, Y.; Zhou, B.; Lu, S.; Wu, Y. Real-World Driving Cycles and Energy Consumption Informed by Large-Sized Vehicle Trajectory Data. *J. Clean. Prod.* **2019**, *223*, 564–574. [CrossRef]
33. Mafi, S.; Kakaee, A.; Mashadi, B.; Moosavian, A.; Abdolmaleki, S.; Rezaei, M. Developing Local Driving Cycle for Accurate Vehicular CO₂ Monitoring: A Case Study of Tehran. *J. Clean. Prod.* **2022**, *336*, 130176. [CrossRef]
34. Sennefelder, R.M.; Micek, P.; Martin-Clemente, R.; Risquez, J.C.; Carvajal, R.; Carrillo-Castrillo, J.A. Driving Cycle Synthesis, Aiming for Realness, by Extending Real-World Driving Databases. *IEEE Access* **2022**, *10*, 54123–54135. [CrossRef]
35. Pan, C.; Gu, X.; Chen, L.; Chen, L.; Yi, F. Driving Cycle Construction and Combined Driving Cycle Prediction for Fuzzy Energy Management of Electric Vehicles. *Int. J. Energy Res.* **2021**, *45*, 17094–17108. [CrossRef]
36. Yuan, M.; Kan, X.; Chi, C.-H.; Cao, L.; Shu, H.; Fan, Y.; Yao, W. Study of Driving Cycle of City Tour Bus Based on Coupled GA-K-Means and HMM Algorithms: A Case Study in Beijing. *IEEE Access* **2021**, *9*, 20331–20345. [CrossRef]
37. Gebisa, A.; Gebresenbet, G.; Gopal, R.; Nallamothe, R.B. Driving Cycles for Estimating Vehicle Emission Levels and Energy Consumption. *Future Transp.* **2021**, *1*, 615–638. [CrossRef]
38. Tzirakis, E.; Pitsas, K.; Zannikos, F.; Stournas, S. Vehicle Emissions and Driving Cycles: Comparison of the Athens Driving Cycle (ADC) with ECE-15 and European Driving Cycle (EDC). *Glob. NEST J.* **2013**, *8*, 282–290. [CrossRef]
39. Chindamo, D.; Gadola, M. What Is the Most Representative Standard Driving Cycle to Estimate Diesel Emissions of a Light Commercial Vehicle? *IFAC Pap.* **2018**, *51*, 73–78. [CrossRef]
40. United Nations Consolidated Resolution on the Construction of Vehicles (R.E.3). Available online: <https://unece.org/fileadmin/DAM/trans/main/wp29/wp29resolutions/ECE-TRANS-WP29-78-r2e.pdf> (accessed on 23 February 2023).
41. Sandrini, G.; Gadola, M.; Chindamo, D. Longitudinal Dynamics Simulation Tool for Hybrid Apu and Full Electric Vehicle. *Energies* **2021**, *14*, 1207. [CrossRef]
42. Electric Vehicle Database—Fiat 500e Hatchback 42 KWh. Available online: <https://ev-database.org/car/1285/Fiat-500e-Hatchback-42-kWh> (accessed on 23 January 2023).
43. FleetNews Electric Car and van Data—Fiat 500e Hatchback 42 KWh Price and Specifications. Available online: <https://www.fleetnews.co.uk/electric-fleet/electric-car-and-van-data/fiat/500e-1285> (accessed on 23 January 2023).
44. MoTeC ADL2—Obsolete. Available online: <https://www.motec.com.au/products/ADL2%20-%20Obsolete?catId=51> (accessed on 16 December 2024).
45. LOCOSYS Technology Inc. Datasheet of GPS Mouse, LS2303x Series. Available online: <https://www.locosystech.com/en/product/gps-mouse-ls2303x.html> (accessed on 26 September 2024).
46. GPS Visualizer. Available online: https://www.gpsvisualizer.com/profile_input (accessed on 26 September 2024).
47. European Parliament and Council Commission Regulation (EU) 2017/1151. Available online: <https://eur-lex.europa.eu/legal-content/EN/TXT/?uri=CELEX:32017R1151> (accessed on 2 October 2024).
48. EPA—United States Environmental Protection Agency EPA US06 or Supplemental Federal Test Procedure (SFTP). Available online: <https://www.epa.gov/emission-standards-reference-guide/epa-us06-or-supplemental-federal-test-procedure-sftp> (accessed on 23 February 2023).
49. EPA—United States Environmental Protection Agency EPA Federal Test Procedure (FTP). Available online: <https://www.epa.gov/emission-standards-reference-guide/epa-federal-test-procedure-ftp> (accessed on 2 May 2023).
50. Japan Inspection Organization-Certification and Inspection Agency in Japan Japanese JC08 Emission Test Cycle. Available online: <https://japaninspection.org/japanese-jc08-emission-test-cycle/> (accessed on 2 May 2023).
51. Common Artemis Driving Cycles (CADC). Available online: <https://dieselnet.com/standards/cycles/artemis.php> (accessed on 28 October 2024).
52. Martyushev, N.V.; Malozyomov, B.V.; Kukartsev, V.V.; Gozbenko, V.E.; Konyukhov, V.Y.; Mikhalev, A.S.; Kukartsev, V.A.; Tynchenko, Y.A. Determination of the Reliability of Urban Electric Transport Running Autonomously through Diagnostic Parameters. *World Electr. Veh. J.* **2023**, *14*, 12. [CrossRef]
53. Das, D.; Ramesha, P.A.; Jana, M.; Basu, S. Generation of Drive Cycles for Electric Vehicles. In Proceedings of the 2021 IEEE Transportation Electrification Conference (ITEC-India), New Delhi, India, 16–19 December 2021; IEEE: New York, NY, USA, 2021; pp. 1–5.

Disclaimer/Publisher’s Note: The statements, opinions and data contained in all publications are solely those of the individual author(s) and contributor(s) and not of MDPI and/or the editor(s). MDPI and/or the editor(s) disclaim responsibility for any injury to people or property resulting from any ideas, methods, instructions or products referred to in the content.